2026 IEEE International Conference on Robotics and Automation (ICRA 2026)
June 1-5, 2026. Vienna, Austria

Design Analysis of Flexible Rod Jamming Based Pneumatically Soft Actuator

Ibrahim A. Seleem[1*,3] and Hiroshi Takemura[2]

***Abstract*— Soft grippers exhibit exceptional adaptability to novel objects and tasks, making them suitable for safe and effective operation in human-centered applications. To improve their stiffness and gripping force, jamming techniques has been frequently used in manipulating objects of diverse shapes and weights. However, the existing jamming based grippers suffer from significant limitations including complex and expensive fabrication, excessive weight, slow recovery response and bending instability due to requiring a high level of vacuum to achieve jamming. This paper presents a novel design of pneumatically actuated flexible rod jamming based soft gripper. It consists of zigzag-based driving chambers to allow bending of the actuator upon pressurization. Additionally, a zigzag jamming chamber filled with flexible rods, that are fabricated by activating the internal support. The design is fabricated completely from Elastic 50A resin using Stereolithography (SLA) fabrication process without the need of additional fabrication procedure. The prototype's stiffness is achieved by regulating the vacuum inside the jamming chamber. A nonlinear static analysis based on 3^{rd} Yeoh model is conducted to investigate the actuator performance in terms of safety and deflection under various operating conditions. The performance of the prototype is evaluated against conventional actuator, while concerning its bending repeatability and payload capacity. The experimental results show that the proposed design achieves bending angle of 178° and carrying external load of 200 g. Additionally, it exhibits low deflection during bending compared to traditional zigzag actuator.**

I. INTRODUCTION

Over the past decade, soft robots have significantly attracted attention in robotic field with a variety of applications including but not limited to soft grippers [1], minimally invasive surgery [2], inspection tasks [3], and space exploration [4]. Unlike traditional robots requiring high accuracy and rigidity, soft robots exhibit inherent compliance and morphological structure, making them adaptable in dynamic environments for safe human-robot interaction.

Robotic grippers are a prominent example of robotic systems that interact with humans and the environment. Compared to rigid grippers driven by motors [5] and Hydraulic actuators [6], soft grippers have shown a promising grasping behavior, offering soft contacts with objects and safe interaction with humans. Additionally, they are fabricated from elastic resins or flexible materials, allowing them mimic human and natural organisms' grasping mechanisms. In recent years, researchers have developed impressive soft grippers with various actuation techniques such as tendons [7], pneumatic actuators [8], Shape Memory Alloy (SMA) [9], and electro-hydraulic actuator [10]. However, the compliance of soft grippers may lead to poor grasping robustness and minimize operational durability, particularly with heavy objects, limiting their use in various applications [11]. To tackle these challenges, variable stiffness soft grippers based on with granular jamming [12], [13], layer jamming [14], [15], and hybrid jamming [16] have been developed. Granular jamming is a widely used technique in which grain-filled elastomeric champers undergo pressure regulation to reversibly conversion between fluid-like and rigid modes [17]. When the reverse pressure is off, the gripper adapts the external shape of the object. On the contrary, its rigid state is achieved by activating reverse pressure, allowing grasping heavy objects.

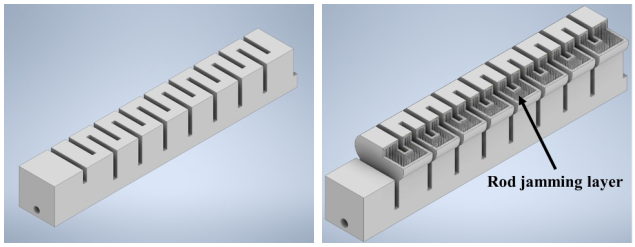

(a) (b)

Fig. 1: (a) Conventional zigzag actuator., and (b) Rod jamming based soft actuator.

Pneumatically actuated Soft gripper based granular jamming was developed in [18]. It was consisted of two champers, one was responsible for bending and the other was filled by glass spheres. Upon pressurizing, the soft actuator achieved bending and exerted pressure on the particle pack, causing the particles within to interlock and jam. In [19], an adaptive variable stiffness soft gripper based on passive particle jamming was proposed. It was composed of three fingers, each has two elastic membrane to enclose the particles inside, that connected through pin joints to two pneumatically actuators. The results showed that these prototypes exhibited variable stiffness under external forces and grasped both soft and rigid objects. However, passive jamming based soft grippers suffer from challenges including limited stiffness variations. In [20], a variables stiffness soft actuator with large bending angle was introduced. It was consisted of driving layer containing a series of connected soft chambers, and

[1*]LIRMM, University of Montpellier, France ibrahim-ali-mohammed.seleem@lirmm.fr
[2]Department of Mechanical and Aerospace Engineering, Faculty of Science and Technology, Tokyo University of Science, Japan takemura@rs.tus.ac.jp
[3]Department of Industrial Electronics and Control Engineering, Faculty of Electronic Engineering, Menoufia University, Egypt (On leave) ebrahim.selim@el-eng.menofia.edu.eg

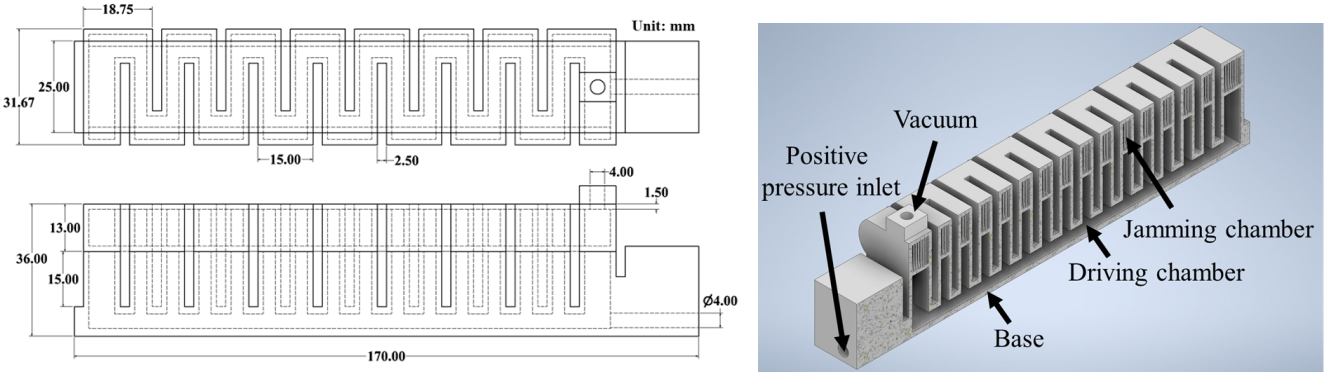

(a) (b)

Fig. 2: (a) Dimensions of variable stiffness based zigzag actuator. and (b) Structural components of the design.

jamming layer. Upon actuation, the design allowed uniform pressure distribution and achieved bending. The jamming layer was activated by applying vacuum and returned back to original state by releasing it. The results demonstrated that the soft gripper performed large bending angle and variable stiffness. A soft robotic gripper with jamming pads for grasping underwater objects based on hydraulic actuation was developed in [21]. The prototype was composed of four fiber-reinforced fluidic elastomeric actuators and two neutrally buoyant jamming pads. The resulting design could grasp objects with a wide range of weights, and geometries. However, soft grippers based on active jamming require high pressure for stiffness modulation. Moreover, they exhibit slow response upon jamming deactivation and tend to be relatively heavy.

It can be concluded that the existing designs of jamming based soft grippers face limitations including but not limited to complex fabrication procedure, bulkiness, bending instability and slow recovery after release jamming. The contributions of our work are summarized in the following aspects:

- Proposing a novel design of variable stiffness based zigzag pneumatic actuator. It consists of a driving layer for bending, and a jamming layer filled with flexible rods. The jamming chamber is produced by activating support step during fabrication of the main actuator, leading to simple and cost-effective fabrication procedure.
- Comparing the payload characteristics of using flexible rod against granular jamming technique including chia seed and glass beads.
- Conducting a Finite Element (FE) simulations using Yeoh nonlinear model to investigate and validate the proposed actuator against traditional zigzag actuator under different operating conditions, while concerning safety and deflection.
- Evaluating the performance of the actuator by carrying out a series of experiments including bending capability, repeatability and payload capacity.

The rest of the paper is organized as follows. A detailed description of the structural design, fabrication and working principle is introduced in Section II. In Section III, Finite Element (FE) simulations of the prototype under different operating conditions is presented. The experimental results and discussion is introduced in Section IV. Section V describes the current challenges and suggested future plans. Finally, the conclusion is presented in Section VI.

II. Structural Design

Soft robotic grippers have adaptive deformation for gripping novel objects due to their inherent compliance. However, external collision or heavy objects may lead to instability during grasping. On the other hand, human hand contains a network of tendinous controlled by the flexor and extensor muscles, which enable the hand to better withstand external collisions [22]. By mimicking this feature, the stiffness of soft grippers can be regulated through programmed stimulus–response mechanisms. Previous attempts have been introduced to control stiffness of soft robotic grippers using self locking mechanism of the exoskeleton structure [23], thermally actuated shape memory polymer [24], layer of stainless steel splint within the finger structure [25], and enclosed layer filled of particles and attached to one side of the actuator [26]. However, those techniques suffer from bulkiness and slow response. In contrast, our design offers a more compact solution in both fabrication and functionality.

Figure 2 illustrates that the design consists of three main components–base, bending and jamming chambers. The length, width and height of actuator are 170 mm, 31.67 mm and 36 mm, respectively. The base layer hosts pressure input of the bending actuation chamber. Unlike traditional PneuNets actuators which were mainly composed of a series of separated chambers, the driving chambers here consists of zigzag configuration to enhance structural stiffness. Additionally, this arrangement also enables the integration of a jamming chamber that is not feasible with traditional PneuNet actuators.

A. Fabrication procedure

Different fabrication methodologies have been carried out to make soft actuators depending on their material. A tra-

ditional Fused Deposition Modeling (FDM) 3D printer that uses thermoplastic materials, such as NinjaFlex, is employed to fabricate the flexible actuators with moderate elasticity [27]. However, the fabricated prototypes require high pressures to achieve bending and/or jamming. Alternatively, molding techniques using silicone-based elastomers, such as Dragon Skin, are widely adopted to achieve higher flexibility and durability [28]. In this technique, a 3D-printed mold is first created, into which the liquid silicone is poured and cured, resulting in a soft actuator with excellent compliance and resilience. Nevertheless, this method is complex, time consuming and lack accuracy. In this article, Stereolithography (SLA) method is utilized for the fabrication of the actuator by focusing an ultraviolet (UV) laser onto photopolymer resin. This method offers enhanced durability and high precision in reproducing fine geometric details, making it particularly suitable for fabricating accurate prototypes [29].

The fabrication procedure is conducted through three stages include printing, cleaning and curing as depicted in Fig. 3. The main machine is the Form 3+ printer, which performs the SLA process by curing Elastic 50 resin layer by layer with a laser beam. After printing, the actuator are transferred to a risning and cleaning unit to remove uncured resin for 15 minutes. Finally, it is placed in a curing machine for 7 minutes under 70 $C°$, where controlled heating and UV exposure are applied to improve their mechanical strength. It is worth mentioning that Elastic 50 resin is selected due to its high elongation and fast return.

Jamming technique is used to provide a variable stiffness to the pneumatic actuator to enable transformation from a flexible to a rigid state by restricting internal motion. It can be achieved by applying negative pressure to create friction and interlocking within the jamming medium. Recently, various jamming approaches were integrated including but not limited to fabric or layer jamming [30], where stacked sheets or fabrics stiffen through increased inter-layer friction

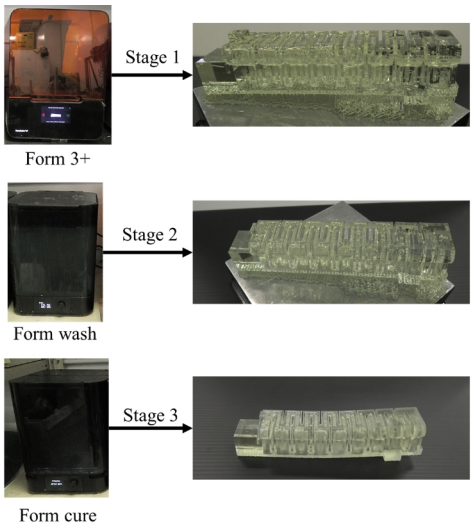

Fig. 3: Fabrication procedure of soft actuator.

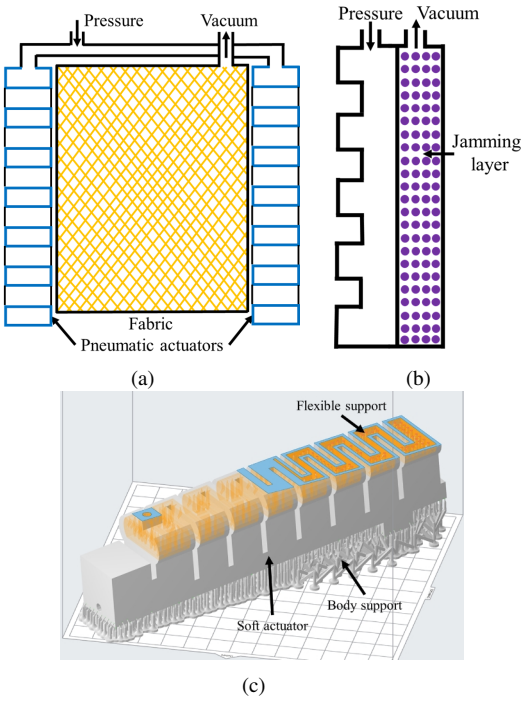

Fig. 4: The jamming approaches including (a) fabric, (b) granular. and (c) soft support.

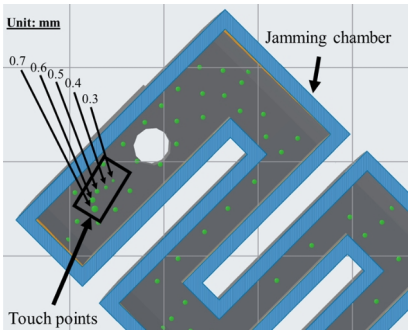

Fig. 5: Adjusting size of touch points for allowing flexibility movement.

as depicted in Fig. 4a. Furthermore, granular jamming is utilized to improve stiffness [31], where natural objects like shia seed or glass particles are implemented inside a membrane lock together under vacuum as shown in Fig. 4b. These methods enable pneumatic actuators to combine high compliance with adjustable rigidity. However, they are still limited by bulkiness and a slow recovery when transitioning from the rigid state to the flexible state.

Here, the jamming layer is composed of flexible rods which is fabricated from similar material of the driving layer to achieve uniformity, reduces fabrication complexity, and enhances recovery response. Figure 4c demonstrates that the jamming chamber is created by enabling support step during the printing procedure, allowing the integration of a fully enclosed jamming chamber directly above the zigzag driving chamber without the need for post-assembly. Each rod is anchored to the jamming chambers through a touch point as

shown in Fig. 5. By adjusting its size, the generated support rods is allowed to be flexible and tightly attached together under applied vacuum for better rigidity. In this paper, the size of touch point is selected to be 0.5 mm. A future plan will be carried out to investigate the effect of modifying the size of touch points on the performance of the prototype.

B. Working Principle

The working principle of the proposed design depends on the combined action of the driving and jamming layers as depicted in Fig. 6. Upon pressurizing the driving layer, the interconnected chambers arranged in a zigzag configuration inflate, generating a smooth bending motion that approximates a circular arc and ensuring uniform deformation along the actuator as shown in Fig. 6b. Figure 6c illustrates that by applying vacuum to the jamming layer, the flexible rods are tightly squeezed to enhances the stiffness of the actuator against external disturbances. Subsequently, the actuator achieves flexible motion and adjustable rigidity.

On the other side, experimental comparison is conducted to evaluate the payload capacity of using flexible rods against other grains such as chia seeds and glass beads. Figures 7a and 7a illustrate that two different configurations are used including cube-shaped and oval-shaped chambers, respectively. Each chamber is individually filled with one of the selected materials and then external loads ranging from 10 g to 140 g are attached to the free end of each chamber. By applying vacuum, it is capable of transition from a soft to rigid state. The weight of each chamber before and after filling with grains is introduced in Table I. Figures 8 illustrates the bending of oval-shaped chamber

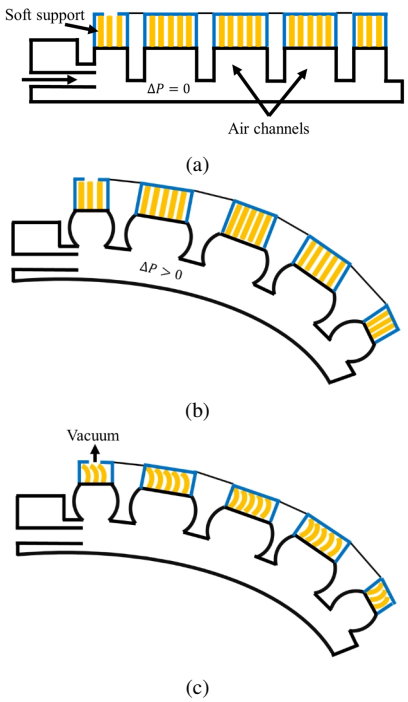

Fig. 6: The working principle of variable stiffness soft actuator.

Configuration	Type	Weight [g]	
		Empty	After filling
Cubic shape	Flexible rod	49	
	Chia seed	38	64
	Glass beads	38	92
Oval shape	Flexible rod	73	
	Chia seed	49	88
	Glass beads	49	92

TABLE I: The weight of jamming chambers.

(a) (b)

Fig. 7: The jamming configurations include (a) Cubic-shaped, and (b) Oval shaped.

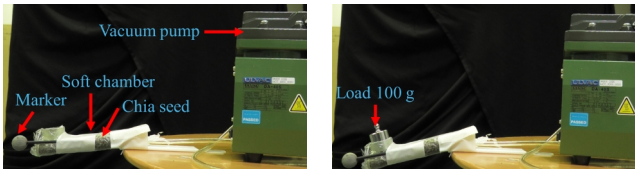

(a) (b)

Fig. 8: The bending shape of oval-shaped chamber after applying vacuum under load 100g.

before and after carrying 100 g, respectively. The deflection of each shape's end is recorded before and after attaching weights using a vision system (OptiTrak). As shown in Fig. 9a and Fig. 9b, the Euclidean distance of each configuration, which represents the norm of the coordinate difference before and after loading, is computed. The results show that chamber with glass beads exhibits higher payload capacity compared to chia seed and flexible rods. However, using grains increases the actuator's weight and lack high recovery response under vacuum. In this article, the oval-shaped is selected due to its superior payload performance and uniform deformation, particularly with the flexible rod. Additionally. it provide relaxed stress concentration compared to sharp edges of cubic shape.

III. Nonlinear Static Analysis

Finite Element Analysis (FEA) are conducted to evaluate the design concept and investigate its mechanical behavior in terms of safety and deflection against traditional zigzag actuator under different operating conditions. A 3^{rd} Yeoh model is selected to describe hyberelastic properties of soft material under large deformations. The strain energy potential is computed as follows:

$$W = \sum_{j=1}^{3} C_j \left(I_1 - 3\right)^j \tag{1}$$

where I_1 is the first invariant of the Cauchy-Green deformation tensor and C_1, C_2 and C_3 represent material coefficients, which are chosen as 0.51495, 0 and 0.003374, respectively, as introduced in [32]. It is worth noting that the material is assumed incompressible.

Three simulation scenarios are performed including zigzag actuator model without a jamming layer. Additionally, the proposed design is analyzed under two conditions including vacuum free and with applying vacuum, respectively. The analysis starts by defining the mechanical properties of Elastic 50 resin with post cured tensile strength of 3.23 MPa [33]. A fixed constraint is applied to the beginning of the actuator. Then, a positive pressure (green arrows) is applied to all inner faces of the driving chamber as shown in Fig. 10. A separation contact is added to each opposite faces of the outer design to avoid overlapping during bending. Figures 11a, 11b and 11c show the resulted stress under applied pressure of 0.03 MPa, 0.055 MPa and 0.079 MPa, respectively. The bending displacement is directly proportional to the applied pressure as depicted in Fig. 14.

Similarly, two simulation scenarios of our proposed design are conducted including deactivation and activation of jamming chamber under pressurizing the driving chamber to investigate the effect of jamming on its bending ability. The pressure distribution of the driving and jamming chambers are shown in Fig. 12. As illustrated in Fig. 13, the stress analysis at both cases under driving pressures of 0.03 MPa, 0.055 MPa and 0.079 MPa, respectively. Figure 14 illustrates that the total displacement while activating the jamming

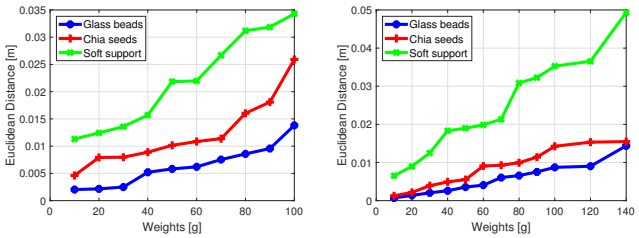

(a) (b)

Fig. 9: The deflection error under external load of (a) Cubic-shaped jamming chamber and (b) oval-shaped jamming chamber.

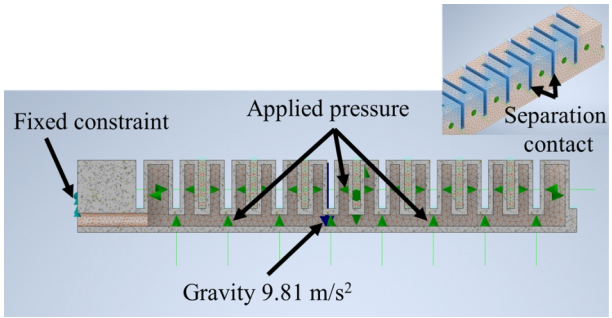

Fig. 10: The applied pressure and constraints of zigzag actuator during the FEA procedure.

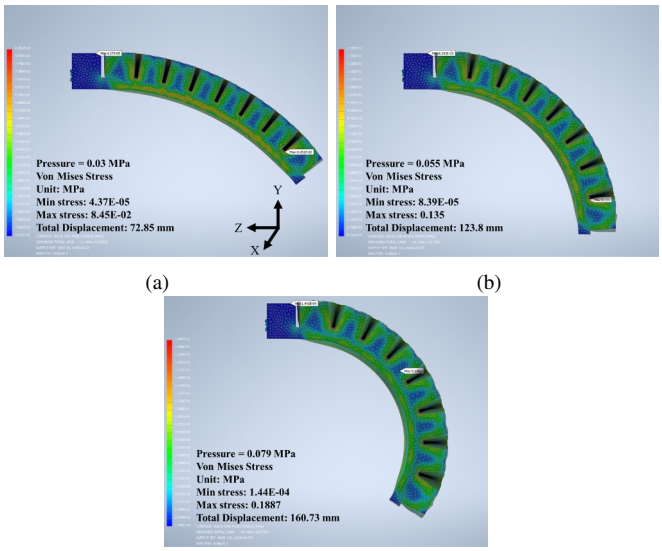

(a) (b)

(c)

Fig. 11: The bending shape of conventional zigzag actuator under applied pressure of (a) 0.03 MPa, (b) 0.055 MPa and (c) 0.079 MPa, respectively.

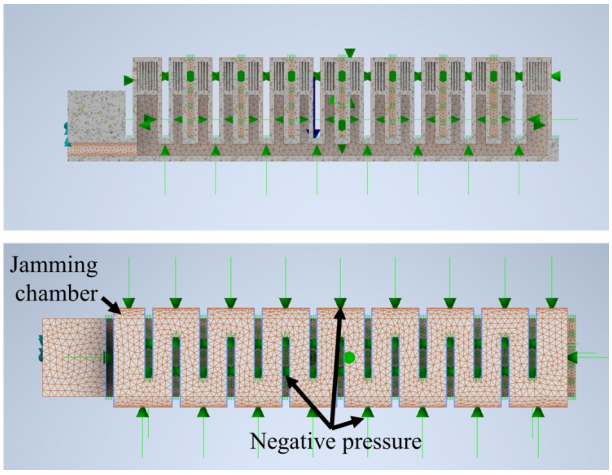

Fig. 12: The FEA's procedure of the proposed actuator.

layer reduces the actuator's bending by approximately 31.7% compared to vacuum free jamming, due to generation of counteracting force against bending. It is worth noting that, pressurizing the driving chamber application of jamming occur simultaneously. However, in the real experiment, the jamming chamber is activated only after achieve bending, resulting in less deflection compared to the simulation analysis. The resulted stress and displacement of the actuator at each simulation scenario are listed in Table. II. The results demonstrate that increasing the applied pressure leads to small deflection of the actuator in X-coordinate.

IV. Results and Discussion

In this section, the performance of proposed prototype is evaluated against traditional zigzag actuator, while concerning its bending, deflection and payload capacity. Figure

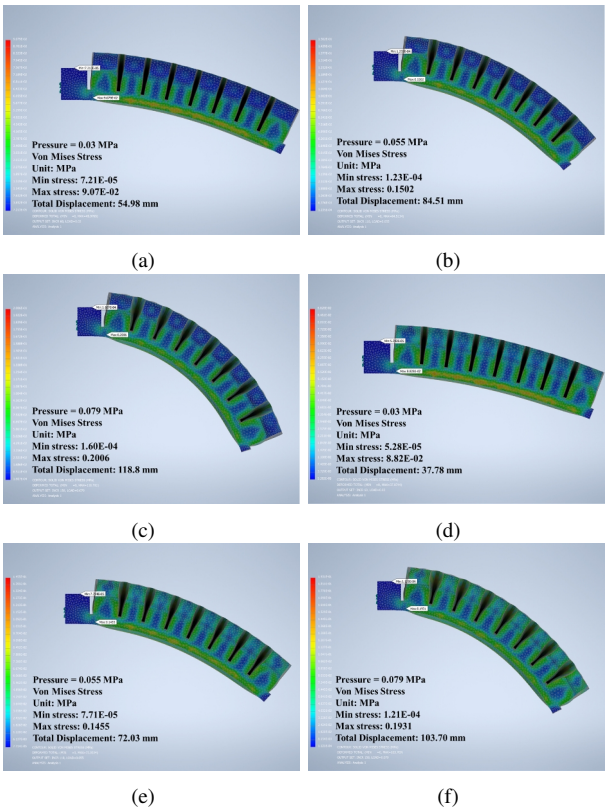

Fig. 13: The stress analysis of the proposed variable stiffness actuator under applied pressure of 0.03 MPa, 0.055 MPa and 0.079 MPa while (a,b,c) deactivating the jamming chambers (d,e,f) activating jamming chambers.

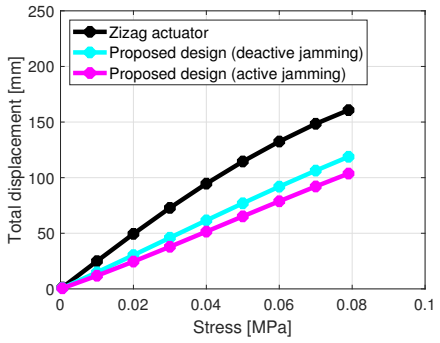

Fig. 14: The resulted displacement under the applied stress.

Model	Applied pressure [MPa]	Von Mises Stress [MPa]		Displacement [mm]						
		Min	Max	X		Y		Z		Total
				min	max	min	max	min	max	
Zigzag actuator	0.03	4.37E-05	8.45E-02	-1.054	1.10	-72.75	0.889	-12.5	17.18	72.85
	0.055	8.39E-05	0.135	-1.96	1.94	-121.7	1.69	-17.37	50.64	123.80
	0.079	1.44E-04	0.188	-2.81	2.69	-148.8	2.51	-20.96	85.6	160.70
Proposed design with deactivated jamming chamber	0.03	7.21E-05	9.07E-02	-0.73	0.97	-43.63	0.51	-15.65	2.62	45.98
	0.055	1.23E-04	0.1502	-1.40	1.72	-83.16	0.89	-21.16	16.36	84.51
	0.079	1.60E-04	0.20	-2.06	2.36	-118.60	1.28	-25.03	31.41	118.8
Proposed design with activated jamming chamber	0.03	5.28E-05	8.82E-02	0.76	0.93	-35.47	0.52	-14.31	0.23	37.87
	0.055	7.74E-05	0.145	-1.467	1.163	-69.94	0.93	-20.88	7.81	72.03
	0.079	1.12E-04	0.1931	-2.17	2.30	-102.9	1.34	-24.53	20.77	103.70

TABLE II: Stresses and displacements of the pneumatic actuator under applied pressure.

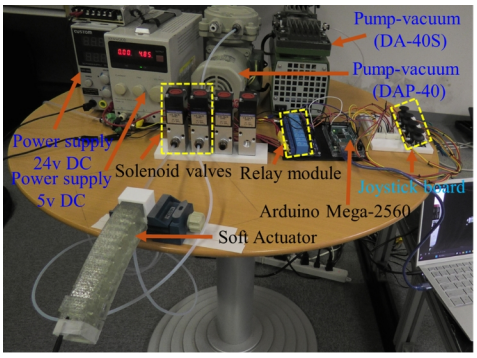

Fig. 15: The experimental setup.

15 illustrates the experimental setup which consists of soft actuator, 24V DC Solenoid valves, pneumatic pump (DA-40S) capable of generating an air pressure of 81.4 kPa and a vacuum pump (DAP-30) with an ultimate pressure of 33.3 kPa, and 5V DC relay board. Additionally, 24 V and 5 V DC power supplies are used to energize solenoid valves and relay drive circuit, respectively. Moreover, a joystick board is utilized to regulate pressure and vacuum by applying Pulse Width Modulation (PWM) through Arduino Mega-2560. The weight of zigzag actuator and our proposed actuator are 73 g and 105 g, respectively.

A. Bending capability

An experimental comparison is carried out to investigate the maximum bending of conventional zigzag-shaped actuator the proposed one, respectively. By, activating the pneumatic pump (DA-40S) through joystick and Arduino board, the zigzag actuator ensures uniform pressure distribution and achieves smooth bending as shown in Fig. 16a and Fig. 16b, respectively. For simplification, the actuator is considered mimicking approximately constant curvature defamation. Its orientation is measured through the body frame, attached to the end-effecor as shown in Fig. 16a. By comparing the recorded orientation to constant curvature assumption, the actuator's bending angle is 341°.

On the other hand, by pressurizing the chambers of our prototype, it tends to bend as depicted in Fig. 17a and Fig. 17b, respectively. Then, by activating the jamming chamber causes the zigzag structure to compress, leading to reduces its overall bending due to the generated a force opposite

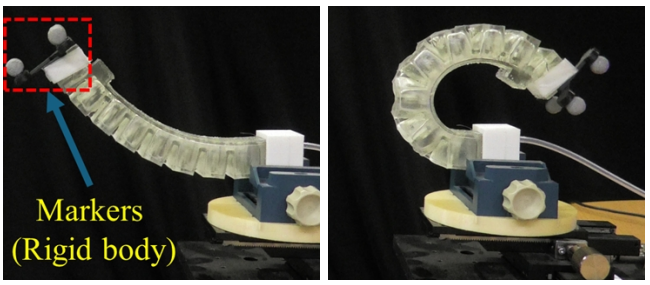

Fig. 16: Bending capability of traditional zigzag actuator.

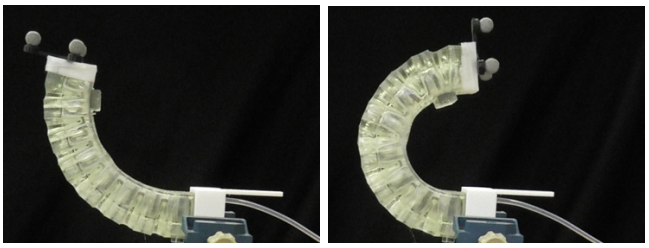

(a) (b)

Fig. 17: The bending of the flexible rod Jamming based soft actuator.

to the bending direction. Similarly, the actuator's can reach 178°.

B. Repeatability

Repeatability represents a key performance metric for robotic systems, reflecting their ability to perform repeated motion with minimal deflection. Additionally, it is critical for precision gripping tasks where reliability and accuracy are required. Repeatability is achieved by allowing the actuator to move repeatedly from start to target positions and measuring its end-effector deviation. Figure 18 illustrates the workspace analysis of the zigzag and our proposed actuators in Cartesian coordinates. The results indicate that the conventional actuator exhibits significant deflection, especially

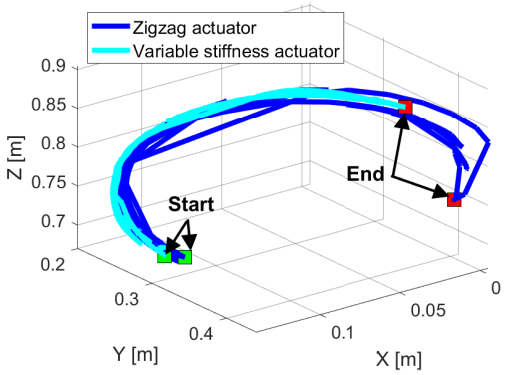

Fig. 18: Workspace reachability of conventional zigzag actuator and variable stiffness based soft actuator.

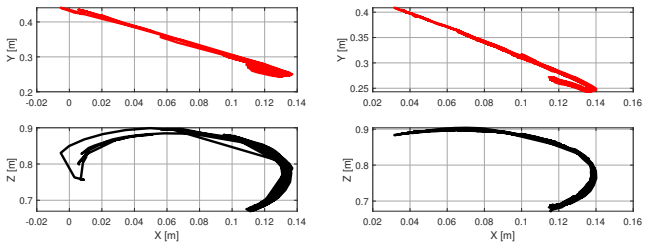

(a) (b)

Fig. 19: The displacement of the (a) traditional zigzag actuator. and (b) variable stiffness actuator.

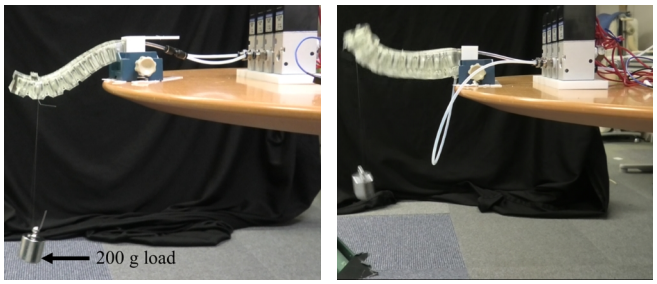

(a) (b)

Fig. 20: The deflection under applied payload of (a) zigzag actuator. and (b) variable stiffness actuator

along the Z-axis as shown in Fig. 19a. On the other side, the proposed prototype demonstrates stable motion with minimal deflection in both the Z- and Y-coordinates as depicted in Fig. 19b depicts, leading to precise grasping tasks.

C. Payload capability

The performance of actuator is investigate under external load, which is significant especially in gripping tasks. In this test, the actuator is allowed to achieve bending while carrying 200 g payload attached to its tip as shown in Fig. 20a. Starting with traditional zigzag actuator, a 200 g is anchored to its end and then by activating pressure inside the chambers, the actuator failed to carry the payload as shown in Fig. 20a. Regarding our proposed actuator, the desired bending is achieved, followed by releasing vacuum from the jamming chamber. Figure 20b illustrates that it is succeeds to carry 200g payload.

V. Challenges and Future Plan

The proposed design show a significant advantageous compared to traditional actuator including low lateral deflection and high payload capacity. However, it suffers high stress concentration at the edges that connects the driving chambers to the base of actuator as depicted in Fig. 21a. Figure 21b illustrates that there are cracks occur during pressurizing the prototype, leading to low durability. In this regards, a future plan is proposed to modify the design by using curved edges to relax the stress and improve its durability. On the other hand, wide range of experiments will be carried out to evaluate design performance under gripping multiple objects.

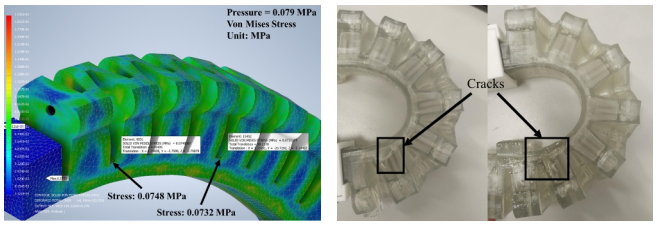

(a) (b)

Fig. 21: (a) Stress concentration at edges of the actuator, (b) Air leakage due to cracks under pressurizing the actuator.

VI. CONCLUSIONS

This paper presents a novel design of flexible rod jamming based zigzag soft actuator for gripping tasks. Comparing to the existing soft grippers that used layer jamming, granular jamming, or metal-based jamming that suffered from excessive size, bending instability, and sophisticated fabrication steps. Our proposed design provide amazing advantageous including compact fabrication procedure, fast recovery response and bending stability. The prototype is composed of driving chamber which is responsible for achieve bending under the applied pressure. Additionally, a jamming chamber which is filled with flexible rods, fabricated by enabling internal support. By activating vacuum, the rods are tightly squeezed to provide varying stiffness. A Finite Element Analysis (FEA) is carried out to investigate the design's bending compared to traditional zigzag actuator. Additionally, experimental validation is conducted to evaluate the prototype's performance, concerning its bending, deflection and payload capacity. The results illustrate that the prototype achieves bending angle of 178° and negligible deflection against conventional actuator. Moreover, it is capable of carry 200 g payload. This paper aims to relax complexity of existing jamming based soft actuator by decreasing fabrication procedure, and improve the stiffness of soft actuators.

REFERENCES

[1] J. Shintake, V. Cacucciolo, D. Floreano, and H. Shea, "Soft robotic grippers," *Advanced materials*, vol. 30, no. 29, p. 1707035, 2018.

[2] V. Consumi, L. Lindenroth, J. Merlin, D. Stoyanov, and A. Stilli, "Design and evaluation of the softscreen capsule for colonoscopy," *IEEE Robotics and Automation Letters*, vol. 8, no. 3, pp. 1659–1666, 2023.

[3] X. Wang, S. Li, J.-C. Chang, J. Liu, D. Axinte, and X. Dong, "Multimodal locomotion ultra-thin soft robots for exploration of narrow spaces," *Nature Communications*, vol. 15, no. 1, p. 6296, 2024.

[4] Y. Zhang, P. Li, J. Quan, L. Li, G. Zhang, and D. Zhou, "Progress, challenges, and prospects of soft robotics for space applications," *Advanced Intelligent Systems*, vol. 5, no. 3, p. 2200071, 2023.

[5] W. Zuo, G. Song, and Z. Chen, "Grasping force control of robotic gripper with high stiffness," *IEEE/ASME Transactions on Mechatronics*, vol. 27, no. 2, pp. 1105–1116, 2021.

[6] Y. Jeong, J. Kim, S. Han, S. Yoon, S. Lee, S. Park, J. T. Kim, J. Kim, and J. Cho, "Design of a hydraulic-driven adaptive gripper with a novel actuation mechanism," *IEEE Robotics and Automation Letters*, 2025.

[7] R. Konda, D. Bombara, S. Swanbeck, and J. Zhang, "Anthropomorphic twisted string-actuated soft robotic gripper with tendon-based stiffening," *IEEE Transactions on Robotics*, vol. 39, no. 2, pp. 1178–1195, 2022.

[8] Z. Zhang, X. Ni, H. Wu, M. Sun, G. Bao, H. Wu, and S. Jiang, "Pneumatically actuated soft gripper with bistable structures," *Soft Robotics*, vol. 9, no. 1, pp. 57–71, 2022.

[9] M. Modabberifar and M. Spenko, "A shape memory alloy-actuated gecko-inspired robotic gripper," *Sensors and Actuators A: Physical*, vol. 276, pp. 76–82, 2018.

[10] T. Park, K. Kim, S.-R. Oh, and Y. Cha, "Electrohydraulic actuator for a soft gripper," *Soft robotics*, vol. 7, no. 1, pp. 68–75, 2020.

[11] C. B. Teeple, J. Werfel, and R. J. Wood, "Multi-dimensional compliance of soft grippers enables gentle interaction with thin, flexible objects," in *2022 International Conference on Robotics and Automation (ICRA)*, pp. 728–734, IEEE, 2022.

[12] P. Jiang, Y. Yang, M. Z. Chen, and Y. Chen, "A variable stiffness gripper based on differential drive particle jamming," *Bioinspiration & biomimetics*, vol. 14, no. 3, p. 036009, 2019.

[13] T. Mitsuda and S. Otsuka, "Active bending mechanism employing granular jamming and vacuum-controlled adaptable gripper," *IEEE Robotics and Automation Letters*, vol. 6, no. 2, pp. 3041–3048, 2021.

[14] Y. Gao, X. Huang, I. S. Mann, and H.-J. Su, "A novel variable stiffness compliant robotic gripper based on layer jamming," *Journal of Mechanisms and Robotics*, vol. 12, no. 5, p. 051013, 2020.

[15] M. Zhu, Y. Mori, T. Wakayama, A. Wada, and S. Kawamura, "A fully multi-material three-dimensional printed soft gripper with variable stiffness for robust grasping," *Soft robotics*, vol. 6, no. 4, pp. 507–519, 2019.

[16] Y. Yang, Y. Zhang, Z. Kan, J. Zeng, and M. Y. Wang, "Hybrid jamming for bioinspired soft robotic fingers," *Soft robotics*, vol. 7, no. 3, pp. 292–308, 2020.

[17] H. Li, J. Sun, and J. M. Herrmann, "Beyond jamming grippers: granular material in robotics," *Advanced Robotics*, vol. 38, no. 11, pp. 715–729, 2024.

[18] Y. Li, Y. Chen, Y. Yang, and Y. Wei, "Passive particle jamming and its stiffening of soft robotic grippers," *IEEE Transactions on robotics*, vol. 33, no. 2, pp. 446–455, 2017.

[19] J. Zhou, Y. Chen, Y. Hu, Z. Wang, Y. Li, G. Gu, and Y. Liu, "Adaptive variable stiffness particle phalange for robust and durable robotic grasping," *Soft robotics*, vol. 7, no. 6, pp. 743–757, 2020.

[20] F. Xu, K. Ma, X. He, M. Wei, and C. Hu, "Design, analysis, and testing of a variable-stiffness soft grabbing robot coupling particle jamming and layer jamming," *Smart Materials and Structures*, vol. 33, no. 5, p. 055036, 2024.

[21] C. E. Capalbo, D. Tomaino, F. Bruno, D. Rizzo, B. Phillips, and S. Licht, "A soft robotic gripper with neutrally buoyant jamming pads for gentle yet secure grasping of underwater objects," *IEEE Journal of Oceanic Engineering*, vol. 47, no. 4, pp. 975–983, 2022.

[22] M. H. Abdelhafiz, L. N. Andreasen Struijk, S. Dosen, and E. G. Spaich, "Biomimetic tendon-based mechanism for finger flexion and extension in a soft hand exoskeleton: design and experimental assessment," *Sensors*, vol. 23, no. 4, p. 2272, 2023.

[23] X.-Y. Guo, W.-B. Li, Q.-H. Gao, H. Yan, Y.-Q. Fei, and W.-M. Zhang, "Self-locking mechanism for variable stiffness rigid–soft gripper," *Smart Materials and Structures*, vol. 29, no. 3, p. 035033, 2020.

[24] Y.-F. Zhang, N. Zhang, H. Hingorani, N. Ding, D. Wang, C. Yuan, B. Zhang, G. Gu, and Q. Ge, "Fast-response, stiffness-tunable soft actuator by hybrid multimaterial 3d printing," *Advanced Functional Materials*, vol. 29, no. 15, p. 1806698, 2019.

[25] C.-Y. Chen, B. W. K. Ang, Y. Li, J. Liu, Z. Liu, and C.-H. Yeow, "Soft printable robots with flexible metal endoskeleton," *IEEE Transactions on Robotics*, vol. 40, pp. 2907–2919, 2024.

[26] Y. Piskarev, A. Devincenti, V. Ramachandran, P.-E. Bourban, M. D. Dickey, J. Shintake, and D. Floreano, "A soft gripper with granular jamming and electroadhesive properties," *Advanced Intelligent Systems*, vol. 5, no. 6, p. 2200409, 2023.

[27] K. Patel, K. Magee, B. Hoover, J. Yu, T. Ashuri, and A. A. Amiri Moghadam, "Development of robotic hand with novel soft 3d printed actuators," in *ASME International Mechanical Engineering Congress and Exposition*, vol. 87622, p. V005T06A060, American Society of Mechanical Engineers, 2023.

[28] A. Bhat, J. W. Ambrose, and R. C.-H. Yeow, "Composite soft pneumatic actuators using 3d printed skins," *IEEE Robotics and Automation Letters*, vol. 8, no. 4, pp. 2086–2093, 2023.

[29] X. Shi, L. Zhang, L. Cheng, C. Xiang, A. Lee, H. Ning, K. Huang, H. Liu, H. Liao, K. An, *et al.*, "Multilayer self-sensing hydrogel soft robot prepared via stereolithography for on-demand drug delivery," *Chemical Engineering Journal*, p. 164352, 2025.

[30] Y. Zhao and Y. Wang, "A palm-shape variable-stiffness gripper based on 3d-printed fabric jamming," *IEEE Robotics and Automation Letters*, vol. 8, no. 6, pp. 3238–3245, 2023.

[31] J. Hu, L. Liang, and B. Zeng, "Design, modeling, and testing of a soft actuator with variable stiffness using granular jamming," *Robotica*, vol. 40, no. 7, pp. 2468–2484, 2022.

[32] C. A. Mendenhall, J. Hardan, T. D. Chiang, L. H. Blumenschein, and A. B. Tepole, "Physics-informed neural network for scalable soft multi-actuator systems," in *2024 IEEE 7th International Conference on Soft Robotics (RoboSoft)*, pp. 716–721, IEEE, 2024.

[33] M. S. Xavier, C. D. Tawk, Y. K. Yong, and A. J. Fleming, "3d-printed omnidirectional soft pneumatic actuators: Design, modeling and characterization," *Sensors and Actuators A: Physical*, vol. 332, p. 113199, 2021.